Journal Pre-proof

An extended macro model accounting for the driver's timid and aggressive attributions and bounded rationality

Zihao Wang, Hongxia Ge, Rongjun Cheng

PII: S0378-4371(19)31689-9
DOI: https://doi.org/10.1016/j.physa.2019.122988
Reference: PHYSA 122988

To appear in: *Physica A*

Received date : 28 June 2019
Revised date : 17 September 2019

Please cite this article as: Z. Wang, H. Ge and R. Cheng, An extended macro model accounting for the driver's timid and aggressive attributions and bounded rationality, *Physica A* (2019), doi: https://doi.org/10.1016/j.physa.2019.122988.

***Highlights (for review)**

1. A new continuum model is presented considering the driver's bounded rationality and behaviors.
2. Applying the linear stability theory, the new model's linear stability is obtained.
3. Through nonlinear analysis, the KdV-Burgers equation is derived.
4. Shock waves, rarefaction waves, stop-and-go waves and local cluster effects can be simulated by the new model.

An extended macro model accounting for the driver's timid and aggressive attributions and bounded rationality

Zihao Wang [1, 2, 3] Hongxia Ge [1, 2, 3] Rongjun Cheng [1, 2, 3†]

[1] Faculty of Maritime and Transportation, Ningbo University, Ningbo 315211, China;

[2] Jiangsu Province Collaborative Innovation Center for Modern Urban Traffic Technologies, Nanjing 210096, China;

[3] National Traffic Management Engineering and Technology Research Centre Ningbo University Sub-centre, Ningbo 315211, China;

Abstract

In this paper, an extended macro traffic flow model is proposed by considering the effects of the driver's bounded rationality and behaviors (e.g., timid and aggressive). The linear stability condition of the model is obtained by linear theory. Through nonlinear analysis, the KdV-Burgers equation is derived, which can reproduce local clusters and stop-and-go waves in the different regions, respectively. Numerical results illustrated that timid behavior inhibit traffic stability, while the effects of driver's route choice behavior and driver's aggressive behavior will enhance traffic stability. Energy consumption is also explored according with above factors. Numerical results indicated that the driver's bounded rationality and aggressive behavior can reduce energy consumption.

Keywords: Macro traffic flow; Energy consumption; Driver's bounded rationality; Driver's timid and aggressive behaviors.

1. Introduction

With the development of vehicle technology and social science, traffic phenomenon (e.g., traffic jam, road overload, average speed drop and traffic energy

† Corresponding author. E-mail: chengrongjun@nbu.edu.cn

consumption, etc.) cannot be neglected any longer. Therefore, researchers are taking various measures [1-5] to solve the increasingly serious traffic problems. In 1956, Richards [6] complemented and refined the LWR model. By combining continuity model and dynamic equation, Payne et al. [7] developed a continuum model with due consideration of the system dynamics, which can solve the problem of boundless acceleration. Previously, Bando et al. [8] proposed an optimal velocity model (OVM), which can counter the free-following and blocking flow. After that, researchers developed several different models, such as car-following model [9-19], cellular automation model [20-24] and route optimization model [25-27] belong to the microscopic model. The hydrodynamic model [28-34] and continuum model [35-41] belong to the macroscopic model. Based on the FVDM proposed by Jiang et al. [8], Jiang et al. [42] further analyzed the structural properties of the solutions of the speed gradient traffic flow model. Tang et al. [43] develop LWR model based on the effects of driver's individual property on his/her perceived density and speed deviation. At the same time, based on the driver's individual difference of the driver's perception ability, Tang et al. [44] develop a new fundamental diagram with the driver's perceived error and speed deviation difference.

In the past studies, we rarely see some models that take into account of both the effects of driver behavior (e.g., timid and aggressive) and driver's bounded rationality. As a matter of fact, different drivers have different drive styles and they usually adjust optimal vehicle velocity according to the change of current traffic conditions. Peng et al. [45] studied an extended model (TAOVM) with consideration of the incorporation timid and aggressive behaviors. Based on the relationship between macro and micro variables, Cheng et al. [38] developed an improved macro traffic flow from the TAOVM. At the same time, with regarding to driver's bounded rationality, which is the driver's choice behavior to adjust the driving route. In other word, when the difference the consumption time on the current route and the optimal route is less than equal to a certain critical value, the driver still runs on the current route. Because he/she thinks the current route is acceptable. The researcher puts forward some traffic flow models to explain driver's bounded rationality [46, 47]. Tang et al. [48] studied

the effect of the driver's bounded rationality on their driving behavior of each vehicle in different traffic conditions, which include the initiation and evolution process of small perturbation). However, the influences of driver's timid and aggressive behaviors are not considered in Tang's model. For this reason, this paper aims to study the influences of driver's bounded rationality on macro driving behavior (e.g., timid and aggressive).

This paper is organized as follows. In Section 2, we proposed the formulation of an improved continuum model considering the effects of aggressive driving, timid driving and driver's bounded rationality, simultaneously. In Section 3, the stability condition of the new macro model is studied. Section 4 discusses the nonlinear stability of the model and the mKdV equation can be got by using nonlinear analysis. And the numerical results will be carried out in Section 5. Finally, we draw conclusions in Section 6.

2. The extended macro traffic flow model

In real traffic, owing to the lack of skilled driving ability and the fear of traffic accidents, most timid drivers tend to drive more carefully. They are typically run slowly and react slowly. By contrast, the experienced drivers can reach their destination in the shortest time. Due to the drivers are divided into two categories, timid and aggressive. Peng et al. [45] put forward a new car-following model as follows:

$$\frac{dv_n(t)}{dt} = a\left[pV\left(\Delta x_n\left(t+\alpha_1\tau\right)\right)+\left(1-p\right)V\left(\Delta x_n\left(t-\alpha_2\tau\right)\right)-v_n\left(t\right)\right]+\lambda\Delta v_n, \qquad (1)$$

where $\Delta v_n = v_{n+1}-v_n$, $a=\frac{1}{\tau}$, λ is the sensitivity coefficient of the speed difference, p is a parameter standing for the intensity between two driver's characteristics, α_1 is the anticipation and reaction delay coefficients of aggressive driving and α_2 is the anticipation and reaction delay coefficients of timid drivers. It

clearly expressed that the drivers perform aggressively when $0.5 \le p \le 1$; when $p = 1$ means the drivers are totally aggressive characteristic. On the contrary, it indicates that the timid behavior became the key impact-factor when $0 \le p \le 0.5$; when $p = 0$ indicates the drivers are wholly conservative characteristic. It means that two types of drivers have the same characteristic as $p = 0.5$.

Cheng et al. [38] developed a new continuum model accounting for the driver's timid and aggressive attributions by using the transformation of macro and micro variable as follows:

$$\frac{dv(x,t)}{dt} = \frac{\partial v}{\partial t} + v\frac{\partial v}{\partial x} = a\left[V_e(\rho) - v\right] + \left[\lambda - (2p-1)\alpha\rho^2 V_e'(\rho)\right]\left(v'(x)\Delta + \frac{\Delta^2}{2}v''(x)\right). \quad (2)$$

Simplifying Eq. (2), we can derive

$$\frac{\partial v}{\partial t} + \left[v - \lambda\Delta + (2p-1)\alpha\rho^2 V_e'(\rho)\Delta\right]\frac{\partial v}{\partial x} = a\left[V_e(\rho) - v\right] + \left[\lambda - (2p-1)\alpha\rho^2 V_e'(\rho)\right]\frac{\Delta^2}{2}v''(x). \quad (3)$$

On the other hand, Tang et al. [49] proposed an extended macro traffic flow model accounting for the driver's bounded rationality as follows:

$$\begin{cases} \rho_t + (\rho v)_x = 0, \\ v_t + v v_x = \begin{cases} 0, & if\ |v_t + v v_x| \le \varepsilon \\ \dfrac{v - V_e(\rho)}{\tau} + c_0 v_x, & otherwise \end{cases} \end{cases} \quad (4)$$

where ε means influence coefficient of driver's bounded rationality, $\tau = \frac{1}{a} = 10s$ is the relaxation time and $c_0 = 10m/s$ is the propagation speed of small perturbation [50].

Next, we proposed a new extended macro traffic flow model, which combines the effect of driver's bounded rationality with timid and aggressive behaviors as follows:

$$\frac{\partial v}{\partial t}+v\frac{\partial v}{\partial x}=\begin{cases}0, & if\ \left|v_t+vv_x\right|\le\varepsilon\\ a\left[V_e(\rho)-v\right]+\left[\lambda-(2p-1)\alpha\rho^2V_e'(\rho)\right]\cdot\left(\Delta v_x+\frac{1}{2}\Delta^2 v_{xx}\right), & otherwise.\end{cases} \tag{5}$$

Note:

(i) When the nth driver's accepts the current speed guidance, the driver will not change the current speed. The stability of the traffic flow remains unchanged.

$$\frac{\partial v}{\partial t}+v\frac{\partial v}{\partial x}=0. \tag{6a}$$

(ii) When the nth driver does not accept the current speed guidance, the driver will immediately adjust his/her speed, so driver will adjust his/her driving behavior, so the driver's acceleration is defined as follows:

$$\frac{\partial v}{\partial t}+v\frac{\partial v}{\partial x}=a\left[V_e(\rho)-v\right]+\left[\lambda-(2p-1)\alpha\rho^2V_e'(\rho)\right]\cdot\left(\Delta v_x+\frac{1}{2}\Delta^2 v_{xx}\right). \tag{6b}$$

3. Linear stability analysis

When $\left|v_t+vv_x\right|\le\varepsilon$, this parameter ε allows the driver to maintain the current speed, avoiding frequent acceleration and deceleration, which makes the flow of vehicles more stable. For this reason, the linear stability analysis was carried out to research the effects of driver's bounded rationality, timid and aggressive behaviors on traffic stability when $\left|v_t+vv_x\right|>\varepsilon$. It is obvious that combining Eq. (6b) with the conservation equation, given as:

$$\begin{cases}\frac{\partial \rho}{\partial t}+\rho\frac{\partial v}{\partial x}+v\frac{\partial \rho}{\partial x}=0,\\ \frac{\partial v}{\partial t}+v\frac{\partial v}{\partial x}=a\left[V_e(\rho)-v\right]+\left[\lambda-(2p-1)\alpha\rho^2V_e'(\rho)\right]\cdot\left(\Delta v_x+\frac{1}{2}\Delta^2 v_{xx}\right).\end{cases} \tag{7}$$

For the sake of facilitate the analytical analysis, we have a vector form of Eq. (7), one gets

$$\frac{\partial \mathbf{U}}{\partial t}+\mathbf{A}\frac{\partial \mathbf{U}}{\partial x}=\mathbf{E}, \tag{8}$$

$$\mathbf{U}=\begin{bmatrix}\rho\\ v\end{bmatrix}, \tag{9}$$

$$\mathbf{A}=\begin{bmatrix}v & \rho\\ 0 & v-\lambda\Delta+(2p-1)\alpha\rho^2V_e'(\rho)\Delta\end{bmatrix}, \tag{10}$$

$$\mathbf{E}=\begin{bmatrix}0\\ a\left[V_e(\rho)-v\right]+\dfrac{\Delta^2}{2}\left(\lambda-(2p-1)\alpha\rho^2V_e'(\rho)v_{xx}\right)\end{bmatrix}. \tag{11}$$

To calculate the eigenvalues of $\mathbf{A}$ by letting the corresponding determinant be zero,

$$\left|\lambda\mathbf{I}-\mathbf{A}\right|=0, \tag{12}$$

where $\mathbf{I}$ is a 2×2 identity matrix. Then, we obtain the following eigenvectors are

$$\lambda_1=v,\quad \lambda_2=v-\lambda\Delta+(2p-1)\alpha\rho^2V_e'(\rho)\Delta. \tag{13}$$

Since $V_e'(\rho)$ is a monotonic decrease function, which is less than zero, obviously the model features the anisotropic property of traffic when $0.5\le p\le1$.

The little disturbance is applied to the homogeneous traffic flow by considering that the steady state is a uniform flow

$$\begin{pmatrix}\rho(x,t)\\ v(x,t)\end{pmatrix}=\begin{pmatrix}\rho_0\\ v_0\end{pmatrix}+\begin{pmatrix}\hat{\rho}_k\\ \hat{v}_k\end{pmatrix}\exp(ikx+\sigma_k t). \tag{14}$$

Substituting Eq. (14) into Eq. (7), then only considered the first and second terms of Taylor's expansion, we can derive

$$\begin{cases}(\sigma_k+v_0ik)\hat{\rho}_k+\rho_0ik\hat{v}_k=0,\\ aV_e'(\rho_0)\hat{\rho}_k+\left[-\dfrac{(k\Delta)^2}{2}\left(\lambda-(2p-1)\alpha\rho_0^2V_e'(\rho_0)\right)-a-\sigma_k-\right.\\ \left.v_0ik+\lambda\Delta ik-(2p-1)\alpha\rho_0^2V_e'(\rho_0)\Delta ik\right]\hat{v}_k=0.\end{cases} \tag{15}$$

When the Eq. (15) entails a non-zero solution, the determinant of the coefficient matrix should be always equal to zero, i.e.

$$\begin{vmatrix}\sigma_k+v_0ik & \rho_0ik\\ aV_e'(\rho_0) & -\dfrac{\lambda(k\Delta)^2}{2}-a-\sigma_k-v_0ik+\lambda\Delta ik+(2p-1)\alpha\rho_0^2V_e'(\rho_0)\Delta k\left(\dfrac{k\Delta}{2}-i\right)\end{vmatrix}=0. \tag{16}$$

By cross multiplying and subtracting, we can get

$$\left(a+\frac{(k\Delta)^2}{2}\left(\lambda-(2p-1)\alpha\rho_0^2V_e'(\rho_0)\right)-\lambda\Delta ik+(2p-1)\alpha\rho_0^2V_e'(\rho_0)\Delta ik\right)\cdot(\sigma_k+v_0ik)+a\rho_0V_e'(\rho)ik$$
$$+(\sigma_k+v_0ik)^2=0. \tag{17}$$

The neutral stability condition for traffic flow can be deduced

$$a=\frac{\lambda\Delta+\rho_0V_e'(\rho_0)}{(2p-1)\Delta\alpha\rho_0^2V_e'(\rho_0)}. \tag{18}$$

Equation (18) clearly demonstrate that the correlation parameter p of two driver's behaviors have a large impact in stabilizing the traffic flow. The neutral stability lines in the parameter space of $(\rho;a)$ are shown in Figure 1. By assigning and modifying the argument value, the stable region is negatively correlated with the parameter value p, which verified that timid driving is worse than aggressive driving. Because the aggressive driver changes lanes to avoid rear-end collision in accordance with the observation of the road ahead. It also proved that aggressive driver behavior can enhance the stability of traffic flow.

From Eq. (17), there exists

$$\mathrm{Im}(\sigma_k)=-k\left[v_0+\rho_0V_e'(\rho_0)\right]+O(k^3). \tag{19}$$

From Eq. (19), the critical velocity at which the disturbance propagates

$$c_0(\rho_0)=v_0+\rho_0V_e'(\rho_0), \tag{20}$$

which have a strong resemblance of those mentioned in Ref [51].

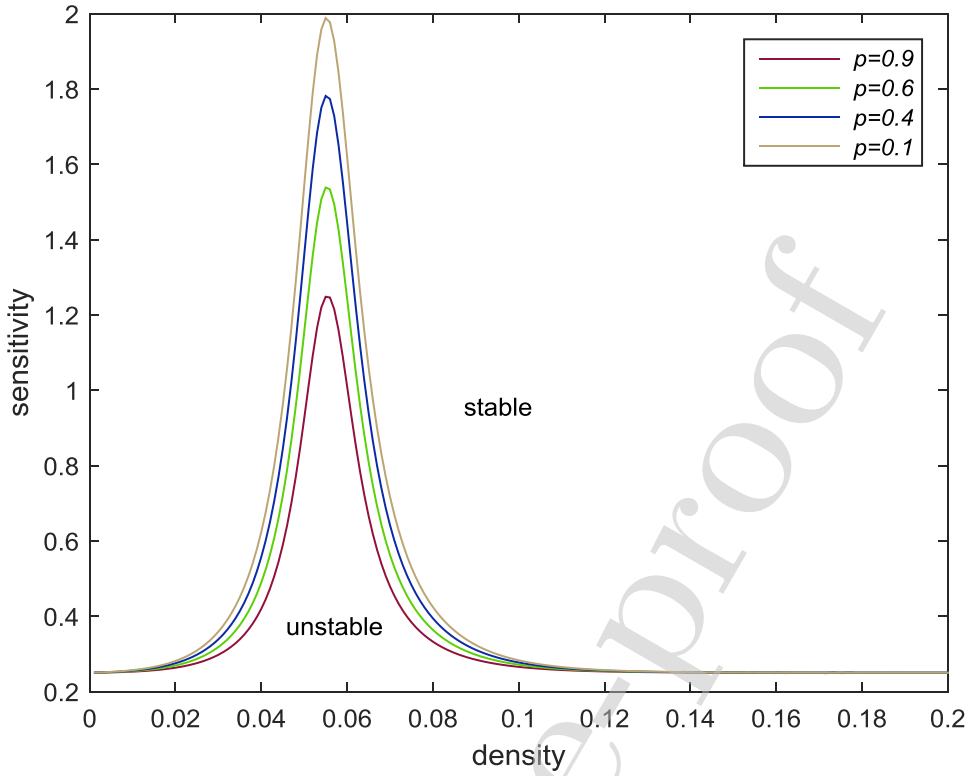

Fig. 1. Neutral stability lines for different intensity influence coefficients p.

4. Nonlinear analysis

Nonlinear analysis is an important component for the entire paper. It often starts from the instability of traffic flow and excavates the internal mechanism of traffic flow state change. Therefore, we employ a new frame of reference as follows [52]:

$$z = x - ct. \tag{21}$$

Applying Eq. (21) into Eq. (7), we have the following normalized equations:

$$\begin{cases} -c\rho_z + q_z = 0, \\ -cv_z + v_z\left(v - \lambda\Delta + (2p-1)\alpha\rho^2 V_e'(\rho)\Delta\right) = a\left[V_e(\rho) - v\right] + \dfrac{\Delta^2}{2}\left(\lambda - (2p-1)\alpha\rho^2 V_e'(\rho)v_{zz}\right). \end{cases} \tag{22}$$

where $q = \rho \cdot v$.

According to Eqs. (21) and (22), we can also get the following derivative equation of v:

$$v_z = \frac{c\rho_z}{\rho} - \frac{q\rho_z}{\rho^2}, \tag{23}$$

$$v_{zz} = \frac{c\rho_{zz}}{\rho} - \frac{2c\rho_z^2}{\rho^2} - \frac{q\rho_{zz}}{\rho^2} + \frac{2q\rho_z^2}{\rho^3}. \tag{24}$$

The flow q is set to the extended expression of the flow

$$q = \rho V_e(\rho) + b_1\rho_z + b_2\rho_{zz}. \tag{25}$$

Substituting Eqs. (23)-(25) into the second formula of Eq. (22) gives

$$\begin{aligned} &-c\left(\frac{c\rho_z}{\rho} - \frac{q\rho_z}{\rho^2}\right) + \left(\frac{q}{\rho} - \lambda\Delta + (2p-1)\alpha\rho^2 V_e'(\rho)\Delta\right)\left(\frac{c\rho_z}{\rho} - \frac{q\rho_z}{\rho^2}\right) \\ &= a\left[V_e(\rho) - \frac{q}{\rho}\right] + \frac{\Delta^2}{2}\left(\lambda - (2p-1)\alpha\rho^2 V_e'(\rho)\right)\left(\frac{c\rho_{zz}}{\rho} - \frac{2c\rho_z^2}{\rho^2} - \frac{q\rho_{zz}}{\rho^2} + \frac{2q\rho_z^2}{\rho^3}\right). \end{aligned} \tag{26}$$

Through balancing the terms ρ_z and ρ_{zz}, the parameters b_1 and b_2 can be acquired as follows:

$$\begin{cases} b_1 = \dfrac{(c - V_e(\rho))\left[c - V_e(\rho) + \Delta\left(\lambda c_0 - (2p-1)\alpha\rho^2 V_e'(\rho)\right)\right]}{1-a}, \\ b_2 = \dfrac{(c - V_e(\rho))\Delta^2\left(\lambda - (2p-1)\alpha\rho^2 V_e'(\rho)\right)}{-2+2a}. \end{cases} \tag{27}$$

Taking $\rho = \rho_h + \hat{\rho}(x,t)$ and using the Taylor series expansions near the neutral stability condition, we obtain:

$$\rho V_e(\rho) \approx \rho_h V_e(\rho_h) + (\rho V_e)_\rho\big|_{\rho=\rho_h}\hat{\rho} + \frac{1}{2}(\rho V_e)_{\rho\rho}\big|_{\rho=\rho_h}\hat{\rho}^2. \tag{28}$$

Putting Eq. (25) with Eq. (28), and turning the $\hat{\rho}$ to ρ, we can obtain

$$-c\rho_z + \left[(\rho V_e)_\rho + (\rho V_e)_{\rho\rho}\rho\right]\rho_z + b_1\rho_{zz} + b_2\rho_{zzz} = 0. \tag{29}$$

In order to obtain accurate KdV-Burgers equation, performing the following transformations:

$$U = -\left[(\rho V_e)_\rho + (\rho V_e)_{\rho\rho}\rho\right], \quad X = mx, \quad T = -mt. \tag{30}$$

Putting Eq. (30) into Eq. (29), we can obtain the KdV–Burgers equation

$$U_T + UU_X - mb_1 U_{XX} - m^2 b_2 U_{XXX} = 0, \tag{31}$$

with analytical solution

$$U = -\frac{3(-mb_1)^2}{25(-m^2 b_2)}\left[\begin{array}{l} 1+2\tanh\left(\pm\frac{-mb_1}{10m^2}\right)\left(X+\frac{6(-mb_1)^2}{25(-m^2b_2)}T+\zeta_0\right) \\ +\tanh^2\left(\pm\frac{-mb_1}{10m^2}\right)\left(X+\frac{6(-mb_1)^2}{25(-m^2b_2)}T+\zeta_0\right) \end{array}\right]. \tag{32}$$

where ζ_0 is an arbitrary constant.

5. Numerical simulation

In this segment, using the numerical simulation of the difference method to study the effects of driver's attributions and bounded rationality in the new continuum model. We also studied whether the proposed new model can smooth out the shock waves and rarefaction waves. Let index i and j represent the space and the time, respectively. The finite difference method was used to discretize Eq. (5) as follow:

$$\rho_i^{j+1} = \rho_i^j + \frac{\Delta t}{\Delta x}\rho_i^j\left(v_i^j - v_{i+1}^j\right) + \frac{\Delta t}{\Delta x}v_i^j\left(\rho_{i-1}^j - \rho_i^j\right). \tag{33}$$

(a) If $\left|\frac{v_i^{j+1}-v_i^j}{\Delta t} + v_i^j\frac{v_{i+1}^j - v_i^j}{\Delta x}\right| \le \varepsilon$

$$v_i^{j+1} = v_i^j. \tag{34}$$

(b) If $\left|\frac{v_i^{j+1}-v_i^j}{\Delta t} + v_i^j\frac{v_{i+1}^j - v_i^j}{\Delta x}\right| > \varepsilon$ and $v_i^j < c_i^j$

$$v_i^{j+1} = v_i^j - \frac{\Delta t}{\Delta x}\left(v_i^j - c_i^j\right)\left(v_{i+1}^j - v_i^j\right) + a\Delta t\left[V_e\left(\rho_i^j\right) - v_i^j\right] - \frac{\Delta t\cdot c_i^j\left(v_{i+1}^j - 2v_i^j + v_{i-1}^j\right)}{2\left(\Delta x\right)^2\cdot\rho_i^j}, \tag{35}$$

(c) If $\left|\frac{v_i^{j+1}-v_i^j}{\Delta t} + v_i^j\frac{v_{i+1}^j - v_i^j}{\Delta x}\right| > \varepsilon$ and $v_i^j \ge c_i^j$

$$v_i^{j+1} = v_i^j - \frac{\Delta t}{\Delta x}\left(v_i^j - c_i^j\right)\left(v_i^j - v_{i-1}^j\right) + a\Delta t\left[V_e\left(\rho_i^j\right) - v_i^j\right] - \frac{\Delta t\cdot c_i^j\left(v_{i+1}^j - 2v_i^j + v_{i-1}^j\right)}{2\left(\Delta x\right)^2\cdot\rho_i^j}, \tag{36}$$

where $c_i^j = \frac{\lambda}{\rho_i^j} - (2p-1)\alpha\rho_i^j V_e'(\rho_i^j)$.

5.1 Shock waves and rarefaction waves

In this section, we conducted a series of numerical experiments to reproduce the evolutions of traffic flow under two typical conditions (i.e., shock wave and rarefaction wave). As pointed out by Daganzo (1995), it is particularly difficult to accurately describe the problem of traffic shock fronts. We explore how the evolution of shock and rarefaction wave under two sets of free boundary conditions, where the initial densities are as follows:

$$\rho_{up}^1 = 0.04veh/m, \quad \rho_{down}^1 = 0.18veh/m, \tag{37a}$$

$$\rho_{up}^2 = 0.18veh/m, \quad \rho_{down}^2 = 0.04veh/m. \tag{37b}$$

where $\rho_{up}^{1,2}$, $\rho_{down}^{1,2}$ are the upstream and downstream initial densities, respectively. Initial speed conditions are

$$v_{up}^{1,2} = v_{r,e}(\rho_{up}^{1,2}), \tag{38a}$$

$$v_{down}^{1,2} = v_{r,e}(\rho_{down}^{1,2}). \tag{38b}$$

Here, we apply the speed-density equilibrium function developed by Castillo et al. [53]:

$$V_e(\rho) = v_f\left[1-\exp\left(1-\exp\left(\frac{c_m}{v_f}\left(\frac{\rho_j}{\rho}-1\right)\right)\right)\right], \tag{39}$$

where c_m is the kinematic wave speed under the jam density and the road length $L = 20km$, $c_m = 11m/s$, $\Delta x = 200m$, $\Delta t = 1s$, $v_f = 30m/s$, $\rho_j = 0.2veh/m$.

The evolution of Eq. (5) can be obtained from Figs. 2 and 3.

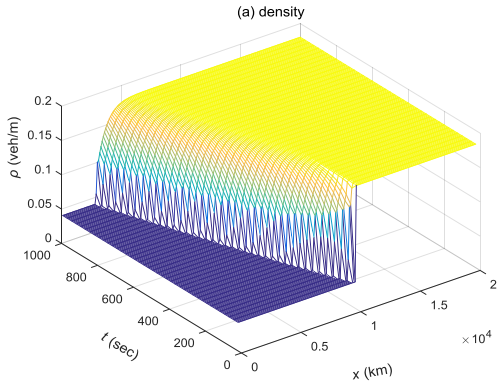

$(a)\ \varepsilon = 0.06$

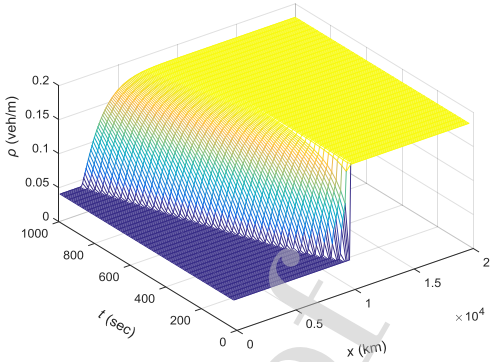

$(b)\ \varepsilon = 0.18$

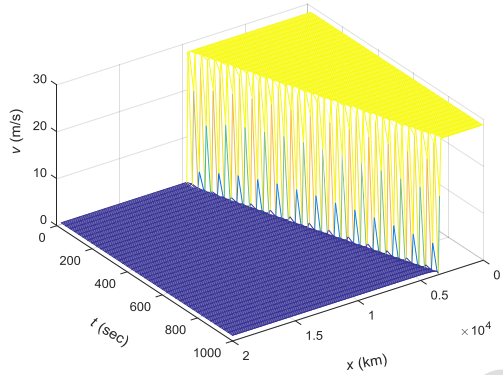

$(c)\ \varepsilon = 0.06$

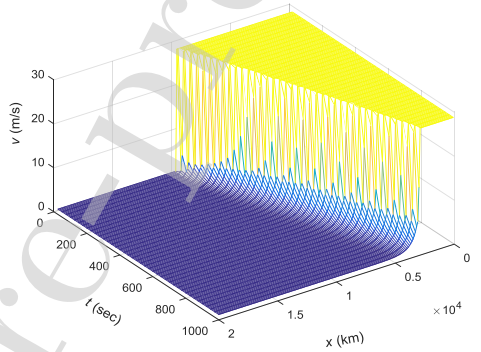

$(d)\ \varepsilon = 0.1$

Fig. 2. Shock waves for different ε under the Riemann initial condition of (37a): temporal development of density (a) $\varepsilon = 0.06$ (b) $\varepsilon = 0.18$; temporal development of speed (c) $\varepsilon = 0.06$ (d) $\varepsilon = 0.18$.

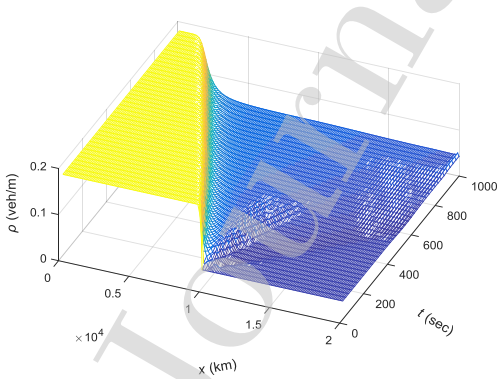

$(a)\ \varepsilon = 0.06$

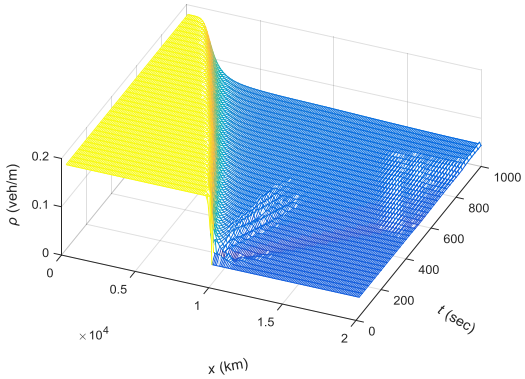

$(b)\ \varepsilon = 0.18$

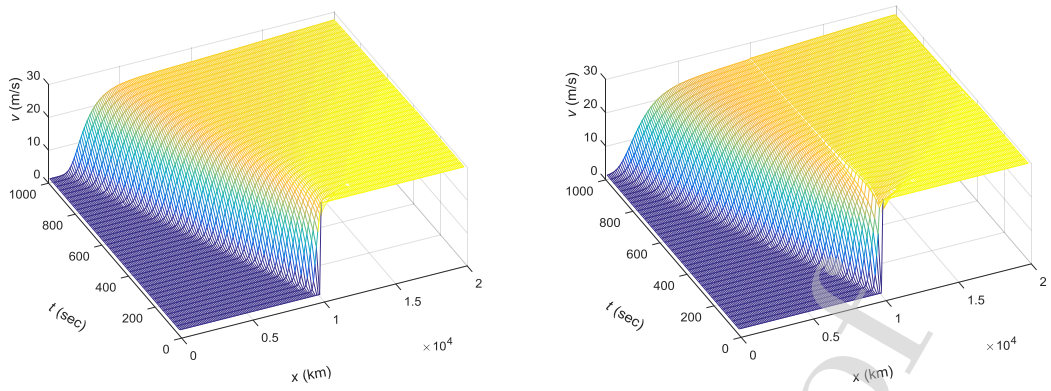

$(c)\varepsilon = 0.06$ $(d)\varepsilon = 0.1$

Fig. 3. Rarefaction waves for different ε under the Riemann initial condition of (37b): temporal development of density (a) $\varepsilon = 0.06$ (b) $\varepsilon = 0.18$; temporal development of speed (c) $\varepsilon = 0.06$ (d) $\varepsilon = 0.18$.

Figs. 2 and 3 display the density and speed evolution of shock and rarefaction wave, respectively. From Figs. 2-3, we have produced conclusive results that our model can effectively describe in enough detail in shock and rarefaction waves. Fig. 2 shows that the wave can be smoother with the increase of the parameter ε, which is agree well with the theoretical analysis. At the same time, the deceleration delay is increasing with the increase of parameter ε, and the trend is the reverse propagation to the vehicle. Fig. 3 shows the rarefaction wave front evolves, which is mainly reflected in shock waves. It can be observed that the wave can be smoothed and form a continuous traffic flow over time.

5.2 Local cluster effect

The new macroscopic model is also used to capture the evolution of small disturbance, just like the well-known as the local cluster effect of traffic flow. The analysis of the local cluster effect can explain the phantom traffic jam in the actual traffic. In this part, we study the phenomenon of local cluster in the process of traffic flow evolution through numerical simulation. Next, we explore the evolution of a small perturbation, where the initial conditions are as follows [54]:

$$\rho(x,0)=\rho_0+\Delta\rho_0\left\{\cosh^{-2}\left[\frac{160}{L}\left(x-\frac{5L}{16}\right)\right]-\frac{1}{4}\cosh^{-2}\left[\frac{40}{L}\left(x-\frac{11L}{32}\right)\right]\right\}, \quad (40)$$

where the road length satisfying $L=32.2km$ and $\Delta\rho_0$ indicates density perturbation. We adopt the boundary condition is periodic, i.e.,

$$\rho(L,t)=\rho(0,t), \quad v(L,t)=v(0,t). \quad (41)$$

By comparing the results in Ref. [55], the balance relationship of the speed and density is expressed as follows:

$$V_e(\rho)=V_f\left[\left(1+\exp\frac{\rho/\rho_m-0.25}{0.06}\right)^{-1}-3.72\times10^{-6}\right], \quad (42)$$

where v_f and ρ_m mean the free flow speed and maximum jam density respectively. What's more, other parameters are here chosen as follows:

$$v_f=30m/s, \quad \rho_m=0.2\,veh/m, \quad \Delta x=100m, \quad \Delta t=1s. \quad (43)$$

5.2.1 Sensitivity to parameter ρ_0

When the parameters are chosen as $p=0.5$, $\varepsilon=0.2$, $\alpha=0.9$, observe the disturbance space-time evolution by changing the initial density value are shown in Fig. 4. In Figure 4, the density fluctuation changes obviously at $\rho_0=0.038veh/m$, $\rho_0=0.058veh/m$, $\rho_0=0.078veh/m$ and $\rho_0=0.098veh/m$, respectively. As shown in Fig. 4, the small perturbation will almost dissipate when the initial traffic density is greater than the upper critical density $0.098veh/m$. As the number of vehicles increase there will be stop-go-stop traffic phenomenon. Therefore, the traffic flow density wave fluctuates drastically with the augment of traffic density (see Fig. 4(a)-(c)).

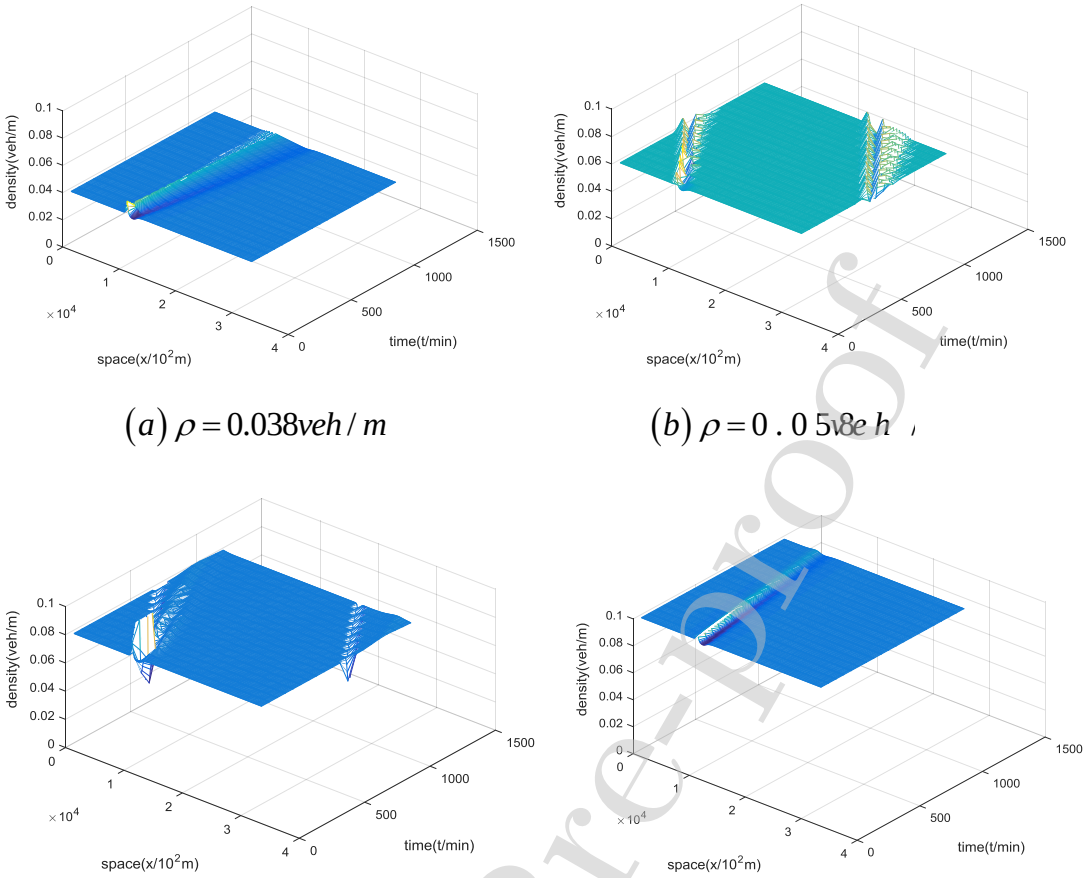

$(a)\ \rho = 0.038 veh/m$ $(b)\ \rho = 0.058 veh/m$

$(c)\ \rho = 0.078 veh/m$ $(d)\ \rho = 0.098 veh/m$

Fig. 4. Spatio-temporal evolution of small perturbation considering the driver's bounded rationality, timid and aggressive behaviors when $p = 0.5$, $\varepsilon = 0.2$, $\alpha = 0.9$ for different initial densities.

5.2.2 Sensitivity to parameter p

Figure 5 represents traffic patterns by considering different influence coefficients of two driver's characteristics for $p = 0.1, 0.4, 0.6, 0.9$ (see Fig. 5(a)-(d)), where $\varepsilon = 0.2$, $\alpha = 0.9$ with initial density $\rho_0 = 0.058\ veh/m$. From Fig. 5, we can find that traffic flow will be more stable with the increase of p. It is concluded that the driver's timid behavior has negative influence on the traffic stability, but the aggressive behaviors' is valuable to reduce traffic jams.

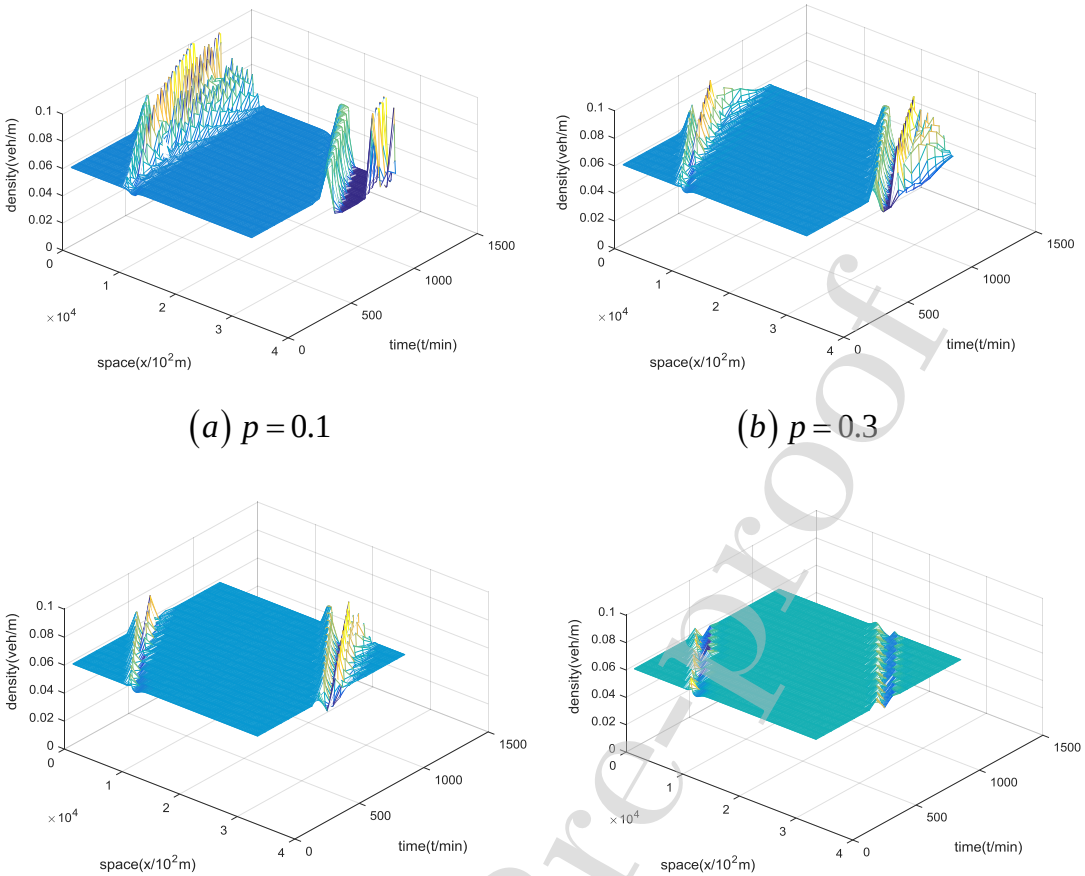

$(a)\ p=0.1$ $(b)\ p=0.3$

$(c)\ p=0.6$ $(d)\ p=0.9$

Fig. 5. Spatio-temporal evolution of traffic flow when $\varepsilon=0.2$, $\alpha=0.9$ with initial density $\rho_0=0.058\ veh/m$ for different intensity influence coefficients p of two driver's characteristics.

5.2.3 Sensitivity to parameter ε

Figure 6 displays the spatio-temporal evolution of traffic density for various arguments ε where $\rho_0=0.058 veh/m$, $\alpha=0.9$ with intensity influence coefficient $p=0.4$. We can clearly see that the amplitude decay with the decrease of ε in free space, which verifies the effect of driver's route choice behavior has positive impact on increasing the traffic flow stability.

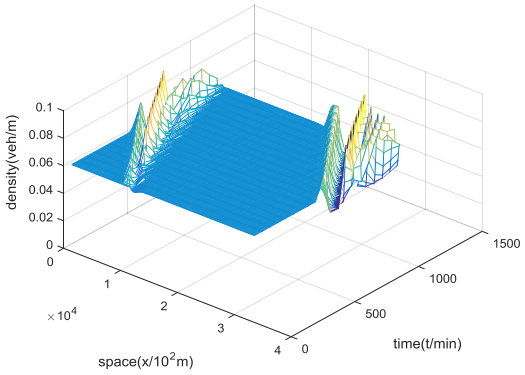

$(a)\ \varepsilon = 0.06$

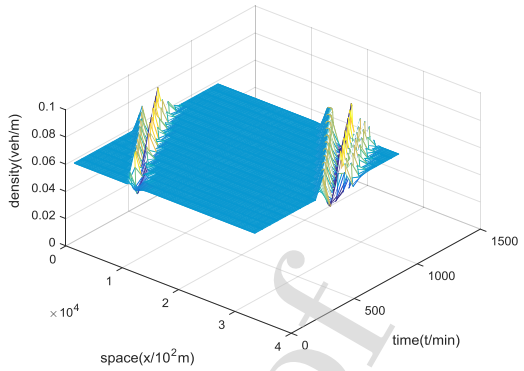

$(b)\ \varepsilon = 0.1$

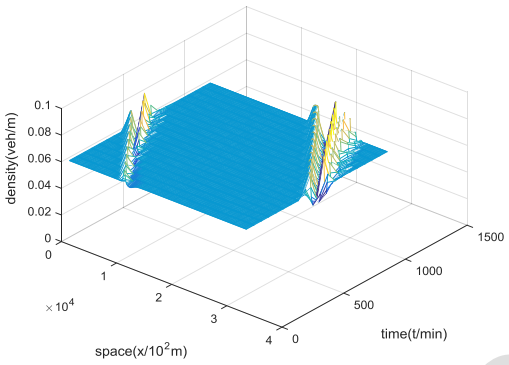

$(c)\ \varepsilon = 0.2$

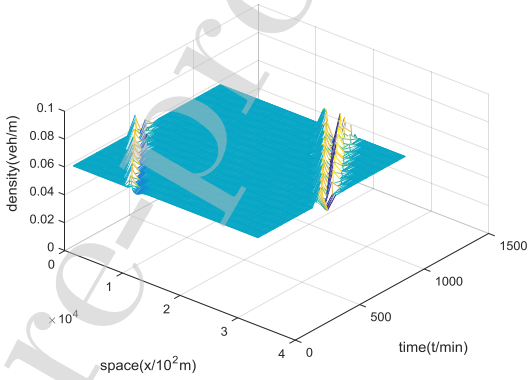

$(b)\ \varepsilon = 0.3$

Fig. 6. Spatio-temporal evolution of density with different ε when $\rho_0 = 0.058 veh/m$, $\alpha = 0.9$ with intensity influence coefficient $p = 0.4$.

5.2.4 Sensitivity to parameter α

Figure 7-8 exhibit the influence of different anticipation ability coefficients α on traffic flow when $\rho_0 = 0.058 veh/m$, $\varepsilon = 0.2$ with $p = 0.4$ and $p = 0.8$, respectively. From Fig. 8, it is clear that the size of density fluctuation decrease gradually with the growth of α when $p > 0.5$, which verifies that the factor of α can effectively anticipation traffic congestions. Conversely, the size of density fluctuation increase gradually with the growth of α when $p < 0.5$ are shown in Fig. 7.

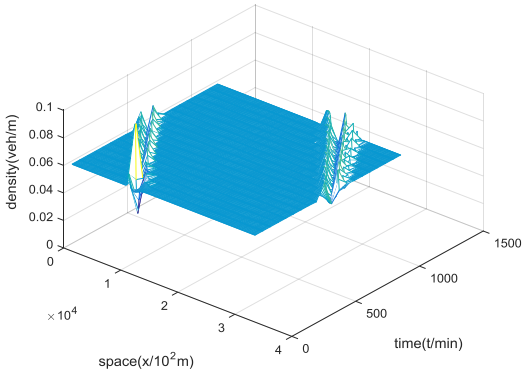

$(a)\ \alpha = 0.1$

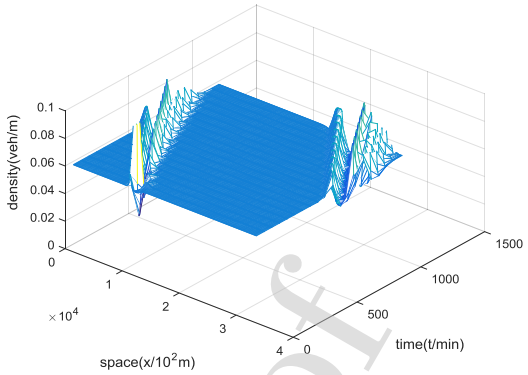

$(b)\ \alpha = 0.4$

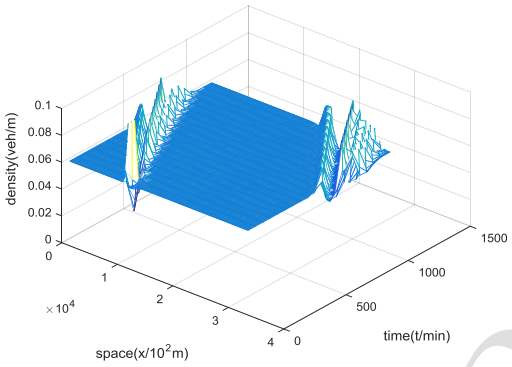

$(c)\ \alpha = 0.6$

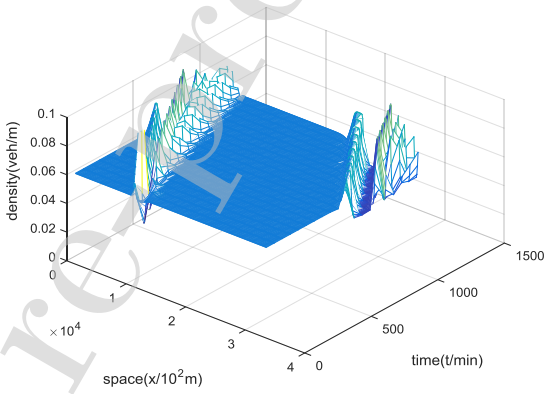

$(d)\ \alpha = 0.9$

Fig. 7. Spatio-temporal evolution of density with different α when $p = 0.4$, $\varepsilon = 0.2$ with initial densities $\rho_0 = 0.058 veh/m$.

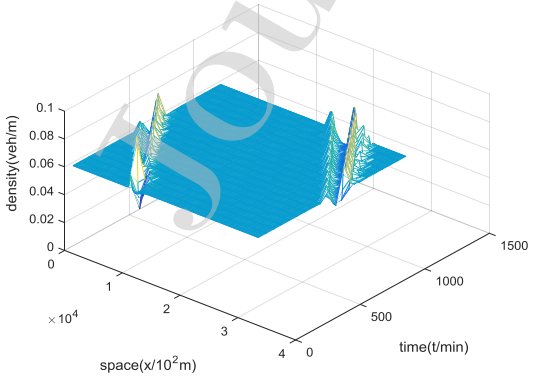

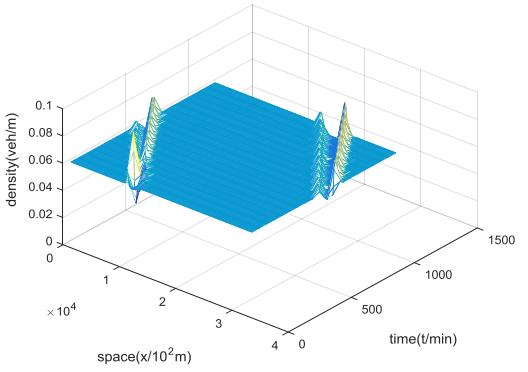

$(a)\ \alpha = 0.1$ $(b)\ \alpha = 0.4$

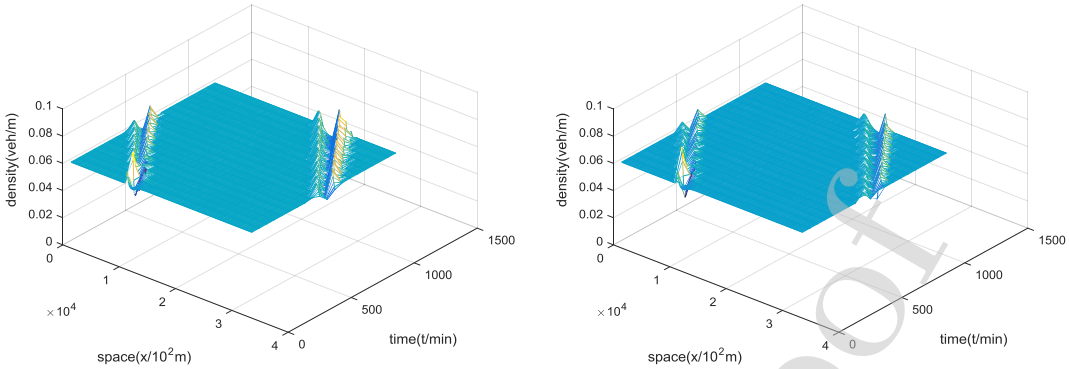

$(c)\ \alpha = 0.6$ $(d)\ \alpha = 0.9$

Fig. 8. Spatio-temporal evolution of density with different α when $p = 0.8$, $\varepsilon = 0.2$ with initial densities $\rho_0 = 0.058 veh/m$.

5.3 Energy consumption

A lot of energy consumption will be caused by acceleration, deceleration and idling in transport system [56-58]. When road conditions, traffic control and traffic members and other factors change, the driving velocity of traffic flow and macro-micro behaviors will change correspondingly, thus affecting the energy consumption of traffic flow. We attempt to explore the effects of driver's attributions and driver's route choice behavior on energy consumption during the whole evolutions in macro traffic flow model. In this paper, the following formula is adopted as energy consumption

$$E(x,t) = \frac{1}{2} v^2(x,t). \tag{44}$$

Here, we apply the fuel consumption change on t and x, it follows that

$$\frac{\partial E(x,t)}{\partial t} = \frac{1}{2} v^2(x,t+\Delta t) - \frac{1}{2} v^2(x,t), \tag{45}$$

$$\frac{\partial E(x,t)}{\partial x} = \frac{1}{2} v^2(x+\Delta x,t) - \frac{1}{2} v^2(x,t), \tag{46}$$

where Δt and Δx is uniform time step and uniform spatial step, respectively.

We study the effect of driver's characteristics on the fuel consumptions during the whole evolutions of small perturbation are given in Fig. 9. Correspondingly, the

energy consumption of vehicle at the mid-position of the space under different p at various time points when $t = 6000\,s$ Figs. 9-10 show that the key variable of driver's characteristics is augment, the car requires less energy to transport within a fixed delay time, which certified that aggressive is more energy efficient than timid driver's behavior.

Figure 11 presents the energy consumption on the road under different parameter α at $t = 6000\,s$. In the meantime, the energy consumption of vehicle at the mid-position of the roadway under different α at various time points are shown in Fig.12. We can see from the Figs. 11-12 that the energy consumption increases proportionally to the element of α when $p < 0.5$. On the other hand, it clearly shown that energy consumption decreases inverse proportion to the element of α when $p > 0.5$. It implies that α can better predict the traffic conditions.

Next, we explore the effect of the driver's bounded rationally on energy consumptions in Fig. 13. From Fig. 13, one can draw a conclusion that the energy consumptions will decrease as the parameter ε increase. It can be known that the driver's bounded rationally can considerably enhance the stability of traffic flow.

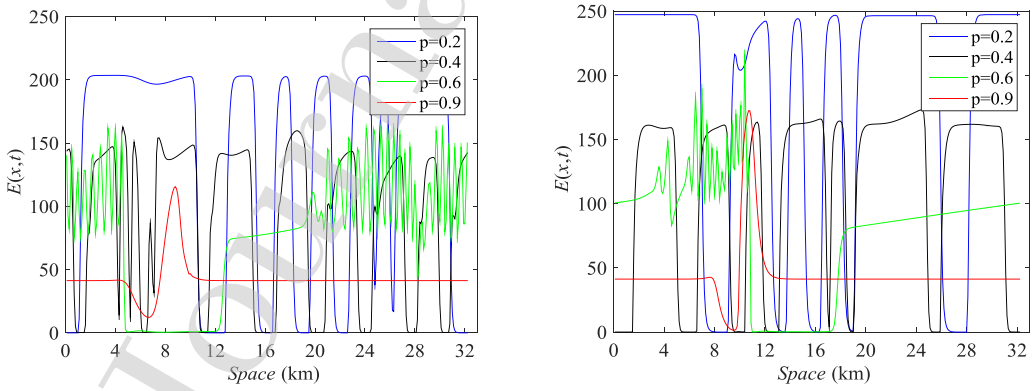

$(a)\ \alpha = 0.$ $(b)\ \alpha = 0.$

Fig. 9. Profile of energy consumption of vehicle with different p at various road points when $t = 6000\,s$, $\rho_0 = 0.06 veh/m$, $\varepsilon = 0.32$.

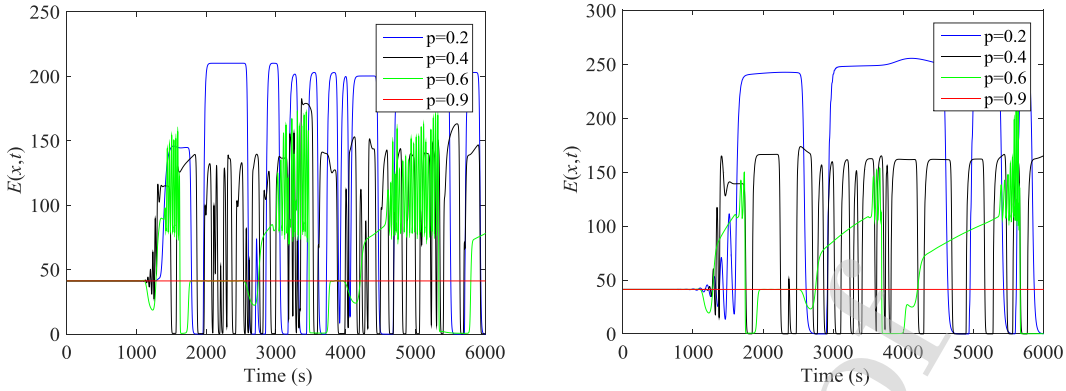

$(a)\ \alpha = 0.4$ $(a)\ \alpha = 0.8$

Fig. 10. Energy consumption of vehicle at the mid-position of the road under different p at various time points when $t = 6000\,s$, $\rho_0 = 0.06veh/m$, $\varepsilon = 0.32$.

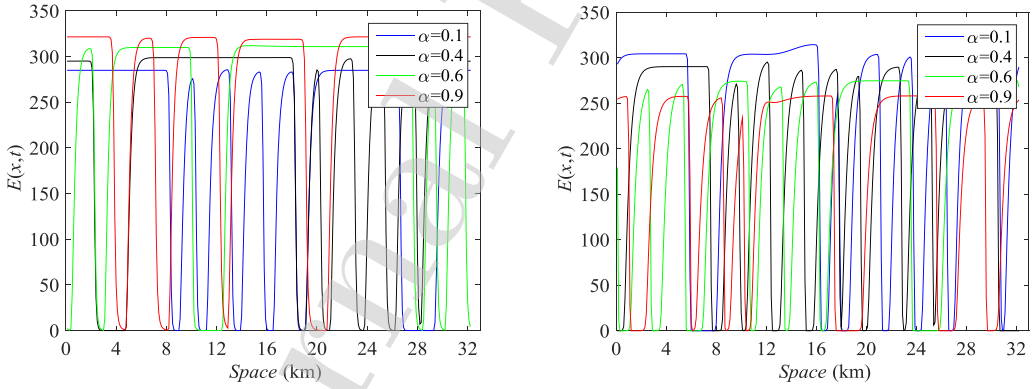

$(a)\ p = 0.4$ $(b)\ p = 0.8$

Fig. 11. Energy consumption of vehicle with different parameter α at various road points when $t = 6000\,s$, $\rho_0 = 0.06veh/m$, $\varepsilon = 0.32$.

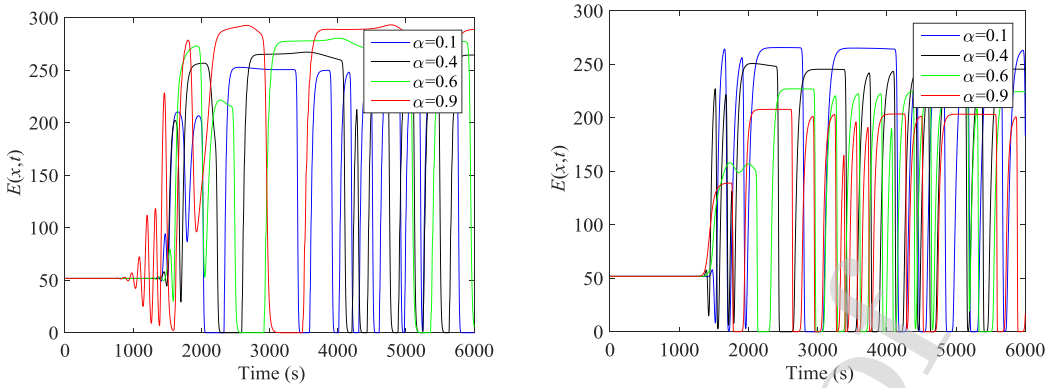

$(a)\ p=0$.　　$(b)\ p=0$.

Fig. 12. Energy consumption of vehicle at the mid-position of the road under different α at various time points when $t=6000\,s$, $\rho_0=0.06veh/m$, $\alpha=0.9$.

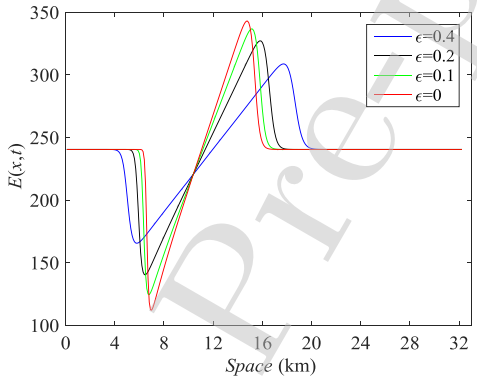

Fig. 13. Energy consumption of vehicle at the mid-position of space x under different ε at various time points when $t=6000\,s$, $p=0.1$, $\varepsilon=0.32$.

6. Conclusion

It is rare to simultaneously explore the impacts of driver's bounded rationality and driver's behavior in existing macro traffic model. This paper firstly construct a new macro continuum model by taking incorporating driver's characteristics and driver's bounded into account. The linear stability condition of the new continuum model under small disturbances is derived. Simulation examples verify that the influences of driver's bounded rationality and driver's attribution (e.g., timed driving and aggressive driving) play an important role in traffic jamming transition. At the same time, the effect of driver's route choice behavior on the propagation of shock

waves and rarefaction waves propagation is explored by the numerical simulations. Energy consumption is also explored for the new model. The analytical and numerical results demonstrate that the impacts of driver's bounded rationality and aggressive driving behavior play an important role in improving the highway capacity and minimizing the vehicle energy consumption.

Acknowledgments

This work is supported by the National Natural Science Foundation of China (Grant No.71571107) and the National Key Research and Development Program of China-Traffic Modeling, Surveillance and Control with Connected &Automated Vehicles (Grant No. 2017YFE9134700) and the K.C. Wong Magna Fund in Ningbo University, China.

References

[1] Z.H. Wang, H.X. Ge, R.J. Cheng, Nonlinear analysis for a modified continuum model considering driver's memory and backward looking effect, Physica A 508(2018)18-27.

[2] Y.F. Li, H. Yang, B. Yang, T.X. Zheng, C. Zhang, An extended continuum model incorporating the electronic throttle dynamics for traffic flow, Nonlinear Dynamics 93(2018)1923-1931.

[3] Z.P. Li, C.Y. Liu, F.Q. Liu, A dynamical model with next-nearest-neighbor interaction in relative velocity, International Journal of Modern Physics C 18(2007)819–832.

[4] W.X. Zhu, L. Jia, Nonliner Analysis of a Synthesized Optimal Velocity Model for Traffic Flow, Communications in Theoretical Physics 50(2008)505.

[5] Z.H. Wang, R.J. Cheng, H.X. Ge, Nonlinear analysis of an improved continuum model considering mean-field velocity difference, Physics Letters A 383(2019)622-629.

[6] P.I. Richards, Shock waves on the highway, Operations Research 4(1956)42-51.

[7] H.J. Payne, Mathematical models of public systems, Simulation Councils Proceedings series 1(1971)51-61.

[8] R. Jiang, Q.S. Wu, Z.J. Zhu, Full velocity difference model for a car-following theory, Physical Review E 64(2001)017101.

[9] J. Zhang, T.Q. Tang, S.W. Yu, An improved car-following model accounting for the preceding car's taillight, Physica A 15(2018)1831-1837.

[10] H.X. Ge, S.Q. Dai, L.Y. Dong, Y. Xue, Stabilization effect of traffic flow in an extended car-following model based on an intelligent transportation system application, Physical Review E 70(2004)066134.

[11] T.Q. Tang, J. He, S.C. Yang, H.Y. Shang, A car-following model accounting for the driver's attribution, Physica A 413(2014)583-591.

[12] W.X. Zhu, H.M. Zhang, Analysis of mixed traffic flow with human-driving and autonomous cars based on car-following model, Physica A 496(2018)274-285.

[13] W.X. Zhu, D. Jun, L.D. Zhang, A compound compensation method for car-following model, Communications in Nonlinear Science and Numerical Simulation 39(2018)427-441.

[14] W.X. Zhu, H.M. Zhang, Analysis of feedback control scheme on discrete car-following system, Physica A 503(2018)322-330.

[15] W.X. Zhu, L.D. Zhang, Analysis of car-following model with cascade compensation strategy, Physica A 449(2018)265-274.

[16] J.J. Zhang, Y.P. Wang, G.Q. Lu, Impact of heterogeneity of car-following behavior on rear-end crash risk, Accident analysis and prevention 125(2019)275-289.

[17] T.Q. Tang, J. Zhang, K. Liu, A speed guidance model accounting for the driver's bounded rationality at a signalized intersection, Physica A 473(2017)45-52.

[18] T.Q. Tang, W.F. Shi, H.J. Huang, W.X. Wu, Z.Q. Song, A route-based traffic flow model accounting for interruption factors, Physica A 514(2019)767-785.

[19] T.Q. Tang, Z.Y. Yi, J. Zhang, T. Wang, J.Q. Leng, A speed guidance strategy for multiple signalized intersections based on car-following model, Physica A 496(2018)399-409.

[20] X.M. Zhou, J.J. Hu, X.F. Jing, X.Z.Y. Xiao, Cellular automaton simulation of pedestrian flow considering vision and multi-velocity, Physica A 514(2019)982-992.

[21] Y.M. Chen, X. Li, X.P. Liu, H, Huang, S.F. Ma, Simulating urban growth boundaries using a patch-based cellular automaton with economic and ecological constraints, International Journal of Geographical Information Science 33(2019)55-80.

[22] L. Wei, Y.Q. Cao, X. Lin, M. Wang, W.D. Huang, Quantitative cellular automaton model and simulations of dendritic and anomalous eutectic growth, Computational Materials Science 156(2019)157-166.

[23] T.Q. Tang, Y.X. Rui, J. Zhang, H.Y. Shang, A cellular automation model accounting for bicycle's group behavior, Physica A 492(2018)1782-1797.

[24] S.Q. Xue, B. Jia, R. Jiang, A behaviour based cellular automaton model for pedestrian counter flow, Journal of Statistical Mechanics: Theory and Experiment 11(2016)113204.

[25] C.X. Ma, W. Hao, A.B. Wang, H.X. Zhao, Developing a coordinated signal control system for urban ring road under the vehicle-infrastructure connected environment, IEEE Access 6(2018)52471-52478.

[26] C.X. Ma, W. Hao, R.C. He, X.Y. Jia, F.Q. Pan, J. Fan, R.Q. Xiong, Distribution path robust optimization of electric vehicle with multiple distribution centers, PLOS ONE 13(2018) e0193789.

[27] C.X. Ma, W. Hao, F.Q. Pan, W. Xiang, Road screening and distribution route multi-objective robust optimization for hazardous materials based on neural network and genetic algorithm, PLOS ONE 13(2018) e0198931.

[28] T. Wang, R.J. Cheng, H.X. Ge, Analysis of a novel lattice hydrodynamic model considering predictive effect and flow integral, Physica A 527(2019)121425.

[29] Q.Y. Wang, H.X. Ge, An improved lattice hydrodynamic model accounting for the effect of "backward looking" and flow integral, Physica A 513(2019)438-446.

[30] R.J. Cheng, Y.N. Wang, An extended lattice hydrodynamic model considering the delayed feedback control on a curved road, Physica A 513(2019)510-517.

[31] Y.Y. Chang, Z.T. He, R.J. Cheng, An extended lattice hydrodynamic model considering the driver's sensory memory and delayed-feedback control, Physica A 514(2019)522-532.

[32] G.H. Peng, H. Kuang, H.Z. Zhao, L. Qing, Nonlinear analysis of a new lattice hydrodynamic model with the consideration of honk effect on flux for two-lane highway, Physica A 515(2019)93-101.

[33] C.T. Jiang, R.J. Cheng, H.X. Ge, Mean-field flow difference model with consideration of on-ramp and off-ramp, Physica A 513(2019)465-467.

[34] C.Q. Zhu, S. Ling, S.Q. Zhong, L.S. Liu, A modified lattice model of traffic flow with the

consideration of the downstream traffic condition, Modern Physics Letters B 33(2019)1950008.

[35] R.J. Cheng, H.X. Ge, J.F. Wang, The nonlinear analysis for a new continuum model considering anticipation and traffic jerk effect, Applied Mathematics and Computation 332(2018)493-505.

[36] Q.T. Zhai, H.X. Ge, R.J. Cheng, An extended continuum model considering optimal velocity change with memory and numerical tests, Physica A 490(2018)774-785.

[37] R.J. Cheng, H.X. Ge, J.F. Wang, An extended macro traffic flow model accounting for multiple optimal velocity functions with different probabilities, Physics Letters A 381(2017)2608–2620.

[38] R.J. Cheng, H.X. Ge, J.F. Wang, An extended continuum model accounting for the driver's timid and aggressive attributions, Physics Letters A 381(2017)1302-1312.

[39] R.J. Cheng, H.X. Ge, J.F. Wang, KdV-Burgers equation in a new continuum model based on full velocity difference model considering anticipation effect, Physica A 481(2017)52–59.

[40] T.Q. Tang, X.F. Luo, J. Zhang, L. Chen, Modeling electric bicycle's lane-changing and retrograde behaviors, Physica A 490(2018)1377-1386.

[41] C. Zhai, W.T. Wu, Analysis of drivers' characteristics on continuum model with traffic jerk effect, Physics Letters A 382(2018)3381-3392.

[42] R. Jiang, Q.S. Wu, Analysis of the structural properties of the solutions to speed gradient traffic flow model, Acta Mechanica Sinica 20(2004)106-112.

[43] T.Q. Tang, Y.P. Wang, G.Z. Yu, H.J. Huang, A Stochastic LWR Model with Consideration of the Driver's Individual Property, Communications in Theoretical Physics 4(2012)583-589.

[44] T.Q. Tang, C.Y. Li, H.J. Huang, H.Y. Shang, A new fundamental diagram theory with the individual difference of the driver's perception ability, Nonlinear Dynamics 67(2012)2255-2265.

[45] G.H. Peng, H.D. He, W.Z. Lu, A new car-following model with the consideration of incorporating timid and aggressive driving behaviors, Physica A 442(2016)197.

[46] X.L. Guo, H.X. Liu, Bounded rationality and irreversible network change, Transportation Research Part B 45(2011)1608.

[47] X. Di, H.X. Liu, J.S. Pang, X.G. Ban, Boundedly rational user equilibria (BRUE): Mathematical formulation and solution sets, Transportation Research Part B 57(2013)300.

[48] T.Q. Tang, H.J. Huang, H.Y. Shang, Influences of the driver's bounded rationality on micro driving behavior, fuel consumption and emissions, Transportation Research Part D 41(2015)423.

[49] T.Q. Tang, G.J. Huang, H.Y. Shang, An extended macro traffic flow model accounting for the driver's bounded rationality and numerical tests, Physica A 468(2017)322–333.

[50] R. Jiang, Q.S. Wu, Z.J. Zhu, A new continuum model for traffic flow and numerical tests, Transportation Research Part B 36(2002)405-419.

[51] D. Helbing, B. Tilch, Generalized force model of traffic dynamics, Physical Review E 58(1998)133-138.

[52] P. Berg, A. Woods, On-ramp simulations and solitary waves of a car-following model, Physical Review E 64(2001)035602.

[53] J.M.D. Castillo, F.G. Benitez, On the function form of the speed-density relationship-I: General theory, Transportation Research Part B 29(1995)373-389.

[54] M. Herrmann, B.S. Kerner, Local cluster effect in different traffic flow models, Physica A 255(1998)163-188.

[55] B.S. Kerner, P. Konhauser, Cluster effect in initially homogeneous traffic flow, Physical Review E 48(1993)2335-2338.

[56] T. Wang, T.Q. Tang, L. Chen, H.J. Huang, Analysis of trip cost allowing late arrival in a traffic corridor with one entry and one exit under car-following model, Physica A 521(2019)387-398.

[57] Y.Q. Sun, H.X. Ge, R.J. Cheng, An extended car-following model considering drivers memory and average aped of preceding vehicles with control strategy, Physica A 521(2019)752-761.

[58] S.C. Yang, C. Deng, T.Q. Tang, Y.S. Qian, Electric vehicle's energy consumption of car-following models, Nonlinear Dynamics 71(2013)323-329.